

Title	Control growth orientation of semipolar GaN layers grown on 3C-SiC/(001) Si
Authors	Dinh, Duc V.;Parbrook, Peter J.
Publication date	2018-08-23
Original Citation	Dinh, D. V. and Parbrook, P. J. [2018] 'Control growth orientation of semipolar GaN layers grown on 3C-SiC/(001) Si', Journal of Crystal Growth, 501, pp. 34-37. doi:10.1016/j.jcrysgr.2018.08.021
Type of publication	Article (peer-reviewed)
Link to publisher's version	10.1016/j.jcrysgr.2018.08.021
Rights	© 2018, Elsevier B.V. All rights reserved. This manuscript version is made available under the CC-BY-NC-ND 4.0 license. - https://creativecommons.org/licenses/by-nc-nd/4.0/
Download date	2024-05-01 06:14:14
Item downloaded from	https://hdl.handle.net/10468/6867

Control growth orientation of semipolar GaN layers grown on 3C-SiC/(001) Si

Duc V. Dinh^{a,*}, Peter J. Parbrook^{a,b}

^a*Tyndall National Institute, University College Cork, Lee Maltings, Dyke Parade, Cork, Ireland*

^b*School of Engineering, University College Cork, Cork, Ireland*

Abstract

Heteroepitaxial growth of GaN buffer layers on 3C-SiC/(001) Si substrates (4°-miscut towards [110]) by metalorganic vapour phase epitaxy has been investigated. High-temperature grown $\text{Al}_x\text{Ga}_{1-x}\text{N}/\text{AlN}$ interlayers were employed to control GaN surface orientations. Semipolar GaN layers with (10 $\bar{1}$ 1), (20 $\bar{2}$ 3) and (10 $\bar{1}$ 2) surface orientations were achieved, as confirmed by x-ray diffraction. Due to the substrate miscut, the growth of (10 $\bar{1}$ 1) layers was twinned along $[\bar{1}\bar{1}0]_{3\text{C-SiC/Si}}$ and $[\bar{1}10]_{3\text{C-SiC/Si}}$ while the growth of (20 $\bar{2}$ 3) and (10 $\bar{1}$ 2) layers was only along $[110]_{3\text{C-SiC/Si}}$. The (10 $\bar{1}$ 1) layers have rough surface morphology while the (20 $\bar{2}$ 3) and (10 $\bar{1}$ 2) layers have mirror-like smooth surface. For all samples with various surface orientations, different photoluminescence peak emission energies were observed at ~ 3.45 eV, 3.78 eV and 3.27 eV at 10 K. These emissions are attributed to the near-band edge of hexagonal GaN, basal-plane stacking faults and partial dislocations, respectively. The dominant luminescence intensity of stacking faults indicates their high density in the GaN layers.

Keywords: A3. Metalorganic vapour phase epitaxy, B1. Nitrides, B2. GaN, B2. Semiconducting aluminium compounds

1. Introduction

Group III-nitride semiconductor compounds have attracted much attention for application in optoelectronic devices. Typically, such devices are epitaxially grown along the [0001] direction; however, the distortion of the crystal lattice introduces a large piezoelectric field, which is detrimental to the performance of the devices. This field can be much reduced along semi- and non-polar directions [1].

Compared to sapphire substrates, silicon (Si) substrates are promising for nitride-based optoelectronic devices due to its low-cost large-diameter wafer, and well-characterized electrical and thermal properties. Different semipolar GaN layers and InGaN/GaN light-emitting diodes (LEDs) have already been prepared on different planar Si substrates such as (10 $\bar{1}$ 2) GaN (with (10 $\bar{1}$ 1) GaN

inclusions) grown on 2-6°-miscut (001) Si [2], (10 $\bar{1}$ 6) LEDs on (112) Si and (10 $\bar{1}$ 5) LEDs on (113) Si [3], as well as (10 $\bar{1}$ 3) GaN [4, 5] and (10 $\bar{1}$ 5) GaN [5] on (001) Si. To improve material quality, patterned Si substrates have also been used to grow semipolar GaN selectively, e.g., (10 $\bar{1}$ 1) GaN on patterned (001) Si [6], (11 $\bar{2}$ 2) GaN on patterned (113) Si [7] and (20 $\bar{2}$ 1) GaN on patterned (114) Si [8]. However, GaN layers on patterned substrates generally have much rougher surfaces compared to layers grown on planar substrates.

For growth of high-quality GaN films, Si substrates are much less suitable due to a large difference in the in-plane thermal expansion coefficients ($5.6 \times 10^{-6} \text{ K}^{-1}$ for GaN and $2.6 \times 10^{-6} \text{ K}^{-1}$ for Si) and a large lattice mismatch (e.g., $\sim 17\%$ between (0001) *c*-plane GaN and (111) Si). This large thermal expansion mismatch generally leads to cracking in GaN layers during cooling from the growth temperature to room temperature. To achieve crack-free GaN on Si, prior to GaN epitaxy, AlN [2, 6, 7] and AlGaIn/AlN interlayers [3] have

*Corresponding author: duc.vn.dinh@gmail.com

Current address: Institute of Materials and Systems for Sustainability, Nagoya University, Nagoya 464-8601, Japan

been employed. Cubic (3C)-SiC has also been used as an intermediate layer for (0001) GaN epitaxy on (111) Si to reduce the lattice and thermal mismatches [9, 10]. Semipolar (10 $\bar{1}2$) GaN layers with 1- μm thickness have been produced on 8°-miscut 3C-SiC/(001) Si with an AlN interlayer by metal-organic vapour phase epitaxy (MOVPE) [11]. However, they are cracked and have a non-uniform surface morphology. Growth of (20 $\bar{2}3$) GaN layer has been attempted on 3C-SiC/(001) Si using hydride-chloride vapour-phase epitaxy [12]. However, the layer consists of oriented grains with size of several tens of microns. Recently, crack-free mirror-like 1.5- μm -thick (20 $\bar{2}3$) GaN layers have been successfully grown on 3C-SiC/(001) Si substrates by MOVPE [13].

In this paper, we report on MOVPE-growth and characterization of GaN layers on 3C-SiC templates, which were prepared on 4°-miscut (001) Si substrates. AlGa $_x$ N/AlN interlayers were optimized to achieve semipolar (10 $\bar{1}1$), (10 $\bar{1}2$) and (20 $\bar{2}3$) surface oriented GaN layers.

2. Experimental

10- μm -thick 3C-SiC templates grown on 4-inch *n*-type (001) Si wafers (4°-miscut towards [110]) using low-pressure hot-wall chemical vapour deposition were produced by Anvil Semiconductors [14, 15]. 100- μm -width polycrystalline SiC grid patterns were used to divide the wafers into square coupons (2.5 \times 2.5 mm 2 size) for stress relief. The full-width at half maximum (FWHM) value of the (002) 3C-SiC symmetric X-ray rocking curve (XRC) of the templates is about 500 arcsec.

Growth of GaN was performed on 3C-SiC/(001) Si substrates in an Aixtron 3 \times 2-inch close-coupled showerhead MOVPE reactor. Ammonia, trimethylaluminium and trimethylgallium were used as precursors. Under a reactor pressure of 50 mbar, the substrates were heated up and thermally cleaned for 2 minutes at $\sim 1100^\circ\text{C}$ in H $_2$ ambient. Afterwards, an approximately 10-nm-thick AlN layer was grown on the substrates at 1100°C . The reactor pressure was increased to 200 mbar during cooling to 950°C corresponding to a growth temperature of AlGa $_x$ N interlayers as measured by a Laytec *in-situ* pyrometer. Approximately 10-nm-thick Al $_x$ Ga $_{1-x}$ N interlayers ($x_{\text{AlN}} \sim 0-0.6$) were grown on the AlN/3C-SiC/Si samples followed by a Si-doped *n*-type GaN over-

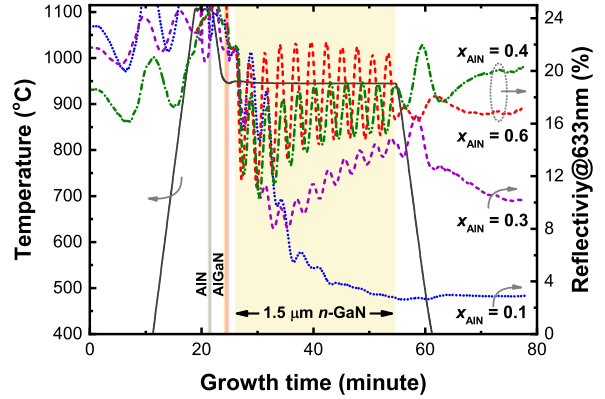


Figure 1: *In-situ* transients of the 633 nm reflectance measured during growth of *n*-type GaN layers grown on 3C-SiC/(001) Si substrates with different Al $_x$ Ga $_{1-x}$ N interlayers.

growth. Growth parameters of Al $_x$ Ga $_{1-x}$ N are reported elsewhere [16].

In-situ analysis was performed using a triple wavelength Laytec EpiTT system giving reflectometry at 405 nm, 633 nm and 950 nm. The crystal orientation and properties of the GaN samples were characterized using a PANalytical X'pert triple-axis high-resolution X-ray diffraction (XRD) system with a CuK $_{\alpha 1}$ source. The surface morphology of the samples was investigated by atomic force microscopy (AFM) in tapping mode (Veeco multimode V) and by Nomarski differential interference contrast microscopy (Olympus XC30). Temperature-dependent photoluminescence (TD-PL) measurements of the samples were performed by a Horiba iHR320 spectrometer using a continuous-wave 244-nm Ar $^{+}$ laser as excitation source.

3. Results and Discussion

Fig. 1 shows *in-situ* transients of the 633 nm reflectance recorded during growth of *n*-type GaN layers grown on the 3C-SiC/(001) Si substrates with different Al $_x$ Ga $_{1-x}$ N/AlN interlayers. For all samples, damping reflectance has been observed that is attributed to a transition from three-dimensional to two-dimensional growth. This damping has been found to decrease with increasing AlN mole fraction of the Al $_x$ Ga $_{1-x}$ N interlayers, suggesting smoother surface morphology. By fitting the Fabry-Pérot oscillations (e.g., for layers grown with $x_{\text{AlN}} \geq 0.4$), the thickness of the layers has been estimated to be (1500 ± 100) nm.

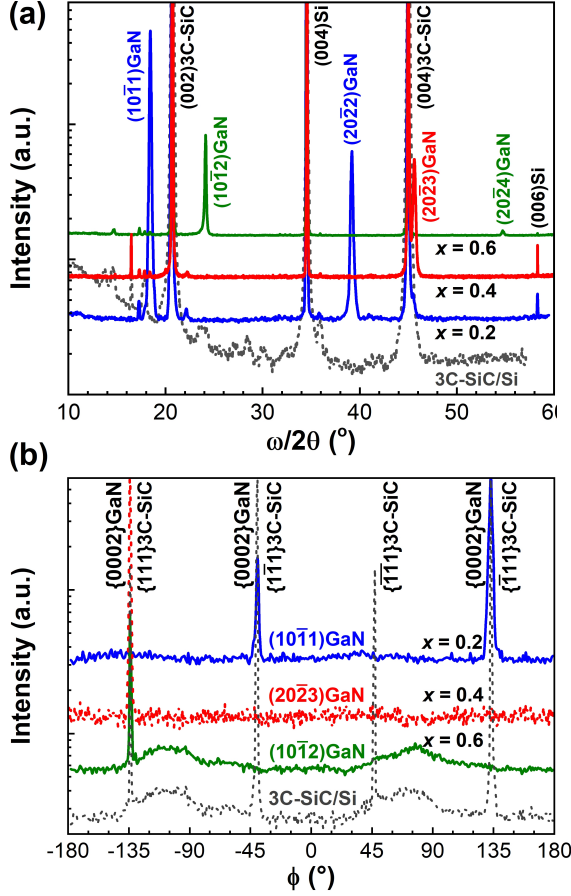


Figure 2: (a) Symmetric $\omega/2\theta$ XRD scans of n -type GaN layers grown on 3C-SiC/(001) Si substrate with different $\text{Al}_x\text{Ga}_{1-x}\text{N}$ interlayers ($x_{\text{AlN}} = 0.2, 0.4$ and 0.6). (b) XRD off-axis ϕ -scans performed in skew-symmetry with settings for the $\{0002\}$ reflection of $(10\bar{1}1)$ GaN ($x_{\text{AlN}} = 0.2$), $(20\bar{2}3)$ GaN ($x_{\text{AlN}} = 0.4$) and $(10\bar{1}2)$ GaN layers ($x_{\text{AlN}} = 0.6$), as well as for the $\{111\}$ reflection of the substrate.

Fig. 2(a) shows symmetric XRD $\omega/2\theta$ scans performed with an open detector of the GaN layers grown on 3C-SiC/(001) Si substrates with different $\text{Al}_x\text{Ga}_{1-x}\text{N}$ interlayers (e.g., $x_{\text{AlN}} = 0.2, 0.4$ and 0.6). An XRD scan of the substrates is also plotted for comparison that shows clearly the 3C-SiC ((002) and (004)) and Si ((004) and (006)) reflections, as well as several reflections from SiC grids (e.g., at about 16 and 36°). For the GaN layers grown with $x_{\text{AlN}} = 0.2, 0.4$ and 0.6 of the interlayers, different dominant reflections are found at about 18.4° , 45.6° and 24.1° , corresponding to the $(10\bar{1}1)$, $(20\bar{2}3)$ and $(10\bar{1}2)$ reflections of GaN, respectively. It has been found that $(10\bar{1}1)$, $(20\bar{2}3)$ and $(10\bar{1}2)$ layers can be grown by the use of three AlN mole fraction ranges

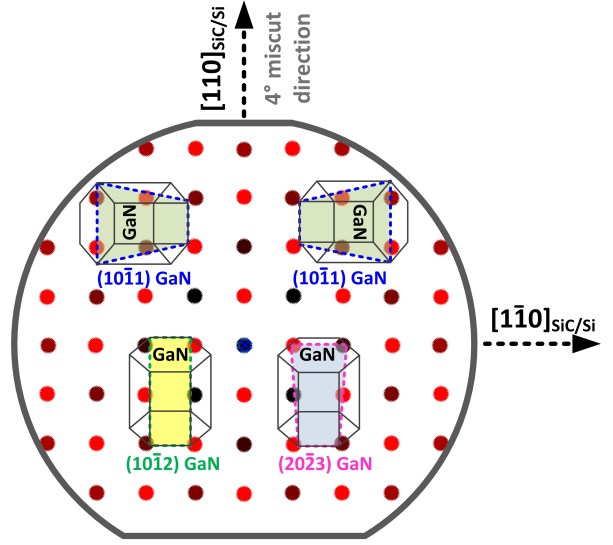


Figure 3: A schematic illustration of three different semipolar $(10\bar{1}1)$, $(10\bar{1}2)$ and $(20\bar{2}3)$ surface oriented GaN possibly grown separately on n -type 3C-SiC/(001) Si (with 4° miscut towards $[110]_{3\text{C-SiC/Si}}$) with three different AlN mole fraction ranges of $x_{\text{AlN}} = 0-0.3, 0.4-0.5$ and $0.5-0.6$ of $\text{Al}_x\text{Ga}_{1-x}\text{N}$ interlayers, respectively.

of $x_{\text{AlN}} = 0-0.3, 0.4-0.5$ and $0.5-0.6$ of the interlayers, respectively. The XRC FWHM value of all GaN layers measured with an open detector without any receiving slit is about 1.0° , indicating their low material quality. This might be due to a propagation of stacking faults from 3C-SiC into the GaN layers [10, 11].

The epitaxial in-plane relationship of the GaN layers with respect to the 3C-SiC/Si substrates was determined from XRD off-axis ϕ -scan. The skew-symmetric $\{111\}$ reflection of (001) 3C-SiC was measured with a tilt angle ($\psi = 54.7^\circ$), which indicates $[110]_{3\text{C-SiC}}$ and $[\bar{1}\bar{1}0]_{3\text{C-SiC}}$. To indicate $[0001]_{\text{GaN}}$ of the $(10\bar{1}1)$, $(10\bar{1}2)$ and $(20\bar{2}3)$ layers, the skew-symmetric $\{0002\}$ reflection was measured with $\psi = 62.0^\circ, 43.2^\circ$ and 54.4° , respectively. As shown in Fig. 2(b), for the $(10\bar{1}2)$ and $(20\bar{2}3)$ layers, only one skew-symmetric $\{0002\}_{\text{GaN}}$ reflection was observed indicating that $[0001]_{\text{GaN}}$ is pointing along $[110]_{3\text{C-SiC}}$. In contrast, for the $(10\bar{1}1)$ layers, two $\{0002\}$ reflections have been observed that rotate by $\pm 90^\circ$ with respect to the $\{0002\}$ reflection of the $(10\bar{1}2)$ and $(20\bar{2}3)$ layers. This indicates a crystalline twinning of the $(10\bar{1}1)$ layers, i.e., $[0001]_{\text{GaN}}$ is pointing along both $[\bar{1}\bar{1}0]_{3\text{C-SiC}}$ and $[110]_{3\text{C-SiC}}$. Fig. 3 shows a schematic illustration of three different $(10\bar{1}1)$,

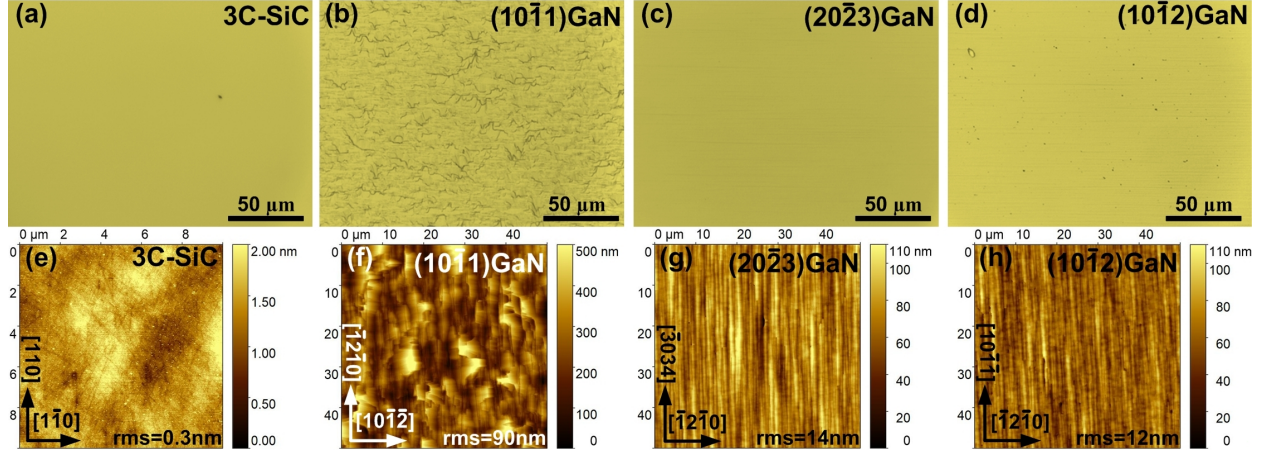


Figure 4: (Top row) Nomarski images of (a) the 3C-SiC/(001) Si substrates, (b) 1.5- μm -thick n -type $(10\bar{1}1)$, (c) $(20\bar{2}3)$ and (d) $(10\bar{1}2)$ GaN layers. (Bottom row) A $20 \times 20 \mu\text{m}^2$ AFM image of the substrates (e) and $50 \times 50 \mu\text{m}^2$ images of the layers grown on the substrates with (f) $(10\bar{1}1)$, (g) $(20\bar{2}3)$ and (h) $(10\bar{1}2)$ GaN surface orientations. Root-mean square (rms) roughness values are shown for comparison.

$(10\bar{1}2)$ and $(20\bar{2}3)$ GaN possibly grown separately on the substrates with three different AlN mole fraction ranges of $x_{\text{AlN}} = 0-0.3$, $0.4-0.5$ and $0.5-0.6$ of $\text{Al}_x\text{Ga}_{1-x}\text{N}$ interlayers, respectively.

For $(10\bar{1}1)$, $(10\bar{1}2)$ and $(20\bar{2}3)$ GaN on (001) 3C-SiC, the lattice mismatch of a -lattice between AlN (GaN) and 3C-SiC is estimated to be about 0.9% (3.4%); the lattice mismatch between c' -lattice of AlN (GaN) and 3C-SiC is estimated to be about -4.1% (-1.2%), -15.4% (-10.2%) and 19.0% (22.9%), respectively. Due to the smallest lattice mismatch, $(10\bar{1}1)$ GaN layers should be always formed on non-miscut substrates and they can be grown equally along four directions of 3C-SiC, i.e., $[110]$, $[\bar{1}\bar{1}0]$, $[\bar{1}\bar{1}0]$ and $[\bar{1}\bar{1}0]$. However, according to the XRD off-axis ϕ -scan (Fig. 2(b)), the $(10\bar{1}1)$ layers were found to grow only along $[110]$ and $[\bar{1}\bar{1}0]$. This is plausible due to the 4° -miscut towards $[110]_{3\text{C-SiC}/\text{Si}}$ of the substrates. This miscut also leads to the $(10\bar{1}2)$ and $(20\bar{2}3)$ layers growing only along $[110]$. Similar findings have previously been observed for $(10\bar{1}2)$ GaN on 2-6 $^\circ$ -miscut (001) Si [2] and on 8 $^\circ$ -miscut 3C-SiC/(001) Si [11].

Fig. 4 shows the surface morphology of 3C-SiC/(001) Si substrates and the n -type GaN layers with $(10\bar{1}1)$, $(20\bar{2}3)$ and $(10\bar{1}2)$ surface orientations. All layers show a crack-free surface. The root-mean square (rms) roughness of the substrates is about 0.3 nm estimated from a $20 \times 20 \mu\text{m}^2$ scan area. The $(10\bar{1}1)$ layers have rough surface morphology with an rms value of ~ 90 nm ($50 \times 50 \mu\text{m}^2$). In con-

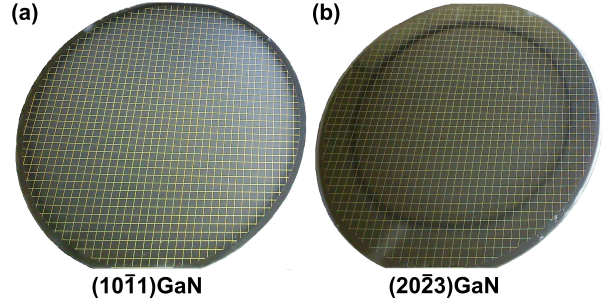


Figure 5: Photographs of the n -type $(10\bar{1}1)$ and $(20\bar{2}3)$ GaN layers grown on 4-inch n -type 3C-SiC/(001) Si wafers.

trast to the $(10\bar{1}1)$ layers, layers with the $(20\bar{2}3)$ and $(10\bar{1}2)$ surface orientations exhibit smooth morphology with similar rms values of ~ 14 nm ($50 \times 50 \mu\text{m}^2$). These latter layers have an undulated morphology along $[\bar{1}2\bar{1}0]_{\text{GaN}}$ due to the anisotropic diffusion of the group-III atoms on these surfaces. Photographs of the $(10\bar{1}1)$ and $(20\bar{2}3)$ GaN layers grown on 4-inch 3C-SiC/(001) Si wafers are shown in Fig. 5, showing a matt surface of the $(10\bar{1}1)$ wafer and a mirror-like surface of the $(20\bar{2}3)$ wafer (and $(10\bar{1}2)$ wafer - not shown). Strong wafer bowing during GaN growth caused the black visible on the $(20\bar{2}3)$ wafer.

TD-PL measurements (10-300 K) were carried out to investigate the optical properties of the GaN layers with different surface orientations. All layers have typical TD-PL spectra as shown in Fig. 6. Different peak emission energies are observed at

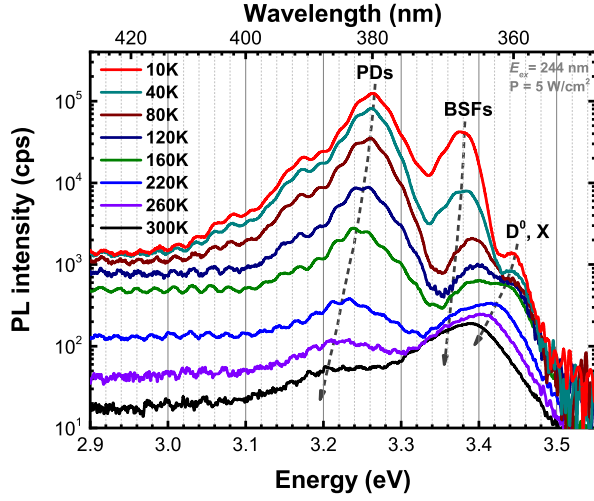


Figure 6: TD-PL spectra of a (10 $\bar{1}2$) GaN layer grown on 3C-SiC/(001) Si substrates.

~ 3.45 eV, 3.38 eV and 3.27 eV at 10 K. They are attributed to the near-band edge of hexagonal GaN (D^0, X), I_1 -type basal-plane stacking faults (BSFs) and partial dislocations (PDs) terminating the BSFs, respectively [17]. The dominant BSF and PD emission intensities indicate their high densities in the layers (i.e., in the range of 10^6 cm^{-1}).

4. Conclusions

Heteroepitaxial MOVPE-growth of crack-free $1.5\text{-}\mu\text{m}$ -thick n -type GaN buffer layers on $\text{Al}_x\text{Ga}_{1-x}\text{N}/\text{AlN}$ interlayers grown on n -type 3C-SiC/(001) Si substrates (4° -miscut towards $[110]$) has been investigated. By adjusting the AlN mole fraction of $\text{Al}_x\text{Ga}_{1-x}\text{N}/\text{AlN}$ interlayers, GaN layers with three different surface orientations have been achieved including (10 $\bar{1}1$), (20 $\bar{2}3$) and (10 $\bar{1}2$). The miscut has been found to cause twins in the (10 $\bar{1}1$) layers along $[\bar{1}\bar{1}0]_{3\text{C-SiC/Si}}$ and $[\bar{1}\bar{1}0]_{3\text{C-SiC/Si}}$, while the growth of (20 $\bar{2}3$) and (10 $\bar{1}2$) layers was only along the miscut direction. The (10 $\bar{1}1$) layers have rough surface morphology, while the (20 $\bar{2}3$) and (10 $\bar{1}2$) layers have mirror-like smooth surface. For all layers, low-temperature PL measurements show dominant stacking fault and dislocation emission intensities indicating their high densities in the layers. Thus, GaN growth conditions need to be further optimized to improve crystallinity.

Acknowledgement

The authors thank Anvil Semiconductors for the provision of the 3C-SiC substrates and their financial support. We also acknowledge the financial support of the EU-FP7 ALIGHT project under agreement no. FP7-280587. PJP acknowledges financial support for his Professorship from Science Foundation Ireland.

References

- [1] T. Takeuchi, S. Sota, M. Katsuragawa, M. Komori, H. Takeuchi, H. Amano, and I. Akasaki, *Jpn. J. Appl. Phys.* **36**, L382 (1997). doi: 10.1143/JJAP.36.L382
- [2] F. Schulze, A. Dadgar, J. Bläsing, and A. Krost, *Appl. Phys. Lett.* **84**, 4747 (2004). doi: 10.1063/1.1760214
- [3] R. Ravash, A. Dadgar, F. Bertram, A. Dempe-wolf, S. Metzner, T. Hempel, J. Christen, and A. Krost, *J. Cryst. Growth* **370**, 288 (2013). doi: 10.1016/j.jcrysgro.2012.08.033
- [4] T. Mitsunari, H. J. Lee, Y. Honda, and H. Amano, *J. Cryst. Growth* **431**, 60 (2015). doi: 10.1016/j.jcrysgro.2015.08.027
- [5] H. J. Lee, S.-Y. Bae, K. Lekkal, A. Tamura, T. Suzuki, M. Kushimoto, Y. Honda, and H. Amano, *J. Cryst. Growth* **468**, 547 (2017). doi: 10.1016/j.jcrysgro.2016.11.116
- [6] T. Murase, T. Tanikawa, Y. Honda, M. Yamaguchi, and H. Amano, *Phys. Status Solidi C* **8**, 2160 (2011). doi: 10.1002/pssc.201000990
- [7] T. Tanikawa, T. Hikosaka, Y. Honda, M. Yamaguchi, and N. Sawaki, *Phys. Status Solidi C* **5**, 2966 (2008). doi: 10.1002/pssc.200779236
- [8] M. Khoury, M. Leroux, M. Nemoz, G. Feillet, J. Zúñiga-Pérez, and P. Vennéguès, *J. Cryst. Growth* **419**, 88 (2015). doi: 10.1016/j.jcrysgro.2015.02.098
- [9] J. Komiyama, Y. Abe, S. Suzuki, and H. Nakanishi, *Appl. Phys. Lett.* **88**, 091901 (2006). doi: 10.1063/1.2175498
- [10] Y. Abe, H. Fujimori, A. Watanabe, N. Ohmori, J. Koriyama, S. Suzuki, H. Nakanishi, and T. Egawa, *J. Jpn. Appl. Phys.* **51**, 035603 (2012). doi: 10.1143/JJAP.51.035603
- [11] Y. Abe, J. Komiyama, T. Isshiki, S. Suzuki, A. Yoshida, H. Ohishi, and H. Nakanishi, *Mater. Sci. Forum* **600**, 1281 (2009). doi: 10.4028/www.scientific.net/MSF.600-603.1281
- [12] L. M. Sorokin, A. E. Kalmykov, A. V. Myasoe-dov, V. N. Bessolov, A. V. Osipov, and S. A. Kukushkin, *J. Phys.: Conf. Ser.* **471**, 012033 (2013). doi: 10.1088/1742-6596/471/1/012033
- [13] D. V. Dinh, S. Presa, M. Akhter, P. P. Maaskant, B. Corbett, and P. J. Parbrook, *Semicond. Sci. Technol.* **30**, 125007 (2015). doi: 10.1088/0268-1242/30/12/125007
- [14] M. Reyes, C. Frewin, P. J. Ward, and S. E. Saddow, *ECS Trans.* **58**, 119 (2013). doi: 10.1149/05804.0119ecst
- [15] Anvil Semiconductors Limited. (<http://www.anvil-semi.co.uk/>)

- [16] D. V. Dinh, S. N. Alam, and P. J. Parbrook, J. Cryst. Growth **435**, 12 (2015). doi: 10.1016/j.jcrysgro.2015.11.009
- [17] J. Lähnemann, U. Jahn, O. Brandt, T. Flissikowski, P. Dogan, and H. T. Grahn, J. Phys. D: Appl. Phys. **47**, 423001 (2014). doi: 10.1088/0022-3727/47/42/423001